

# Hydrogen spillover to enhance hydrogen storage—study of the effect of carbon physicochemical properties

Angela D. Lueking<sup>a,\*</sup>, Ralph T. Yang<sup>b</sup>

<sup>a</sup> Department of Energy and Geo-Environmental Engineering, 120 Hosler, Pennsylvania State University, University Park, PA 16802-5000, USA

<sup>b</sup> Department of Chemical Engineering, 2300 Hayward, University of Michigan, Ann Arbor, MI 48109, USA

Received 3 September 2003; received in revised form 19 January 2004; accepted 21 January 2004

Available online 17 March 2004

## Abstract

Hydrogen storage in carbon materials can be increased by hydrogen spillover from a supported catalyst; a systematic investigation of various carbon supports was used to better understand how hydrogen spillover affects hydrogen storage on carbon materials. Secondary spillover experiments effectively eliminated experimental variables associated with primary spillover, evidenced by materials clustering around the carbon type for a variety of supported catalyst-carbon mixtures. Providing a supported catalyst to act as a hydrogen source enhances the overall hydrogen uptake of a carbon material; for example, simple mixing of carbon nanotubes with supported palladium increased the uptake of the carbons by a factor of three. However, the baseline adsorption of the carbon was the predominant factor in the magnitude of the overall hydrogen uptake, even when hydrogen spillover was active. Three observations illustrated that a dynamic steady-state model is needed for predictive capacity of hydrogen spillover.

© 2004 Elsevier B.V. All rights reserved.

**Keywords:** Hydrogen spillover; Hydrogen storage; Single-wall carbon nanotubes; Multi-wall carbon nanotubes; Graphite nanofibers

## 1. Introduction

Carbon nanotubes are thought to be a promising candidate for hydrogen storage. Recently, the likely role of residual metals in subsequent hydrogen uptake has been brought to light [1,2]. The presence of metals that are capable of hydrogen uptake does not necessarily mean that the carbon is inactive. Hydrogen spillover from metals to carbon surfaces is well documented [3,4] and ab initio molecular orbital studies have shown adsorption of hydrogen atoms is exothermic and stable on the graphite basal plane [5]. The spillover of hydrogen involves a transfer of electrons to acceptors within the support; this process not only modifies the chemical nature of the support but can also activate a previously inactive material and/or induce subsequent hydrogen physisorption [6].

The fundamental hydrogen spillover concepts were established in the late 1960s and 1970s; hydrogen spillover has been reviewed several times, most recently by Conner and

Falconer [7]. Dissociation of hydrogen on a metal and subsequent spillover to its support is highly dependent upon the chemical bridges formed at the interface, either carbon bridges [8] or proton acceptors [9,10]. Hydrogen spillover can be assessed in a number of ways, but perhaps the most common is simple calculation of the hydrogen to metal ratio, either the surface metal ( $M_S$ ) or total metal ( $M_T$ ) content. When spillover occurs, the  $H:M_S$  will typically exceed unity; in the case of materials that form hydrides, the  $H:M_T$  will exceed the stoichiometric ratio of the hydride.

Most mechanistic studies of hydrogen spillover have been onto oxide supports, and oxygen groups are generally thought to act as receptors for spillover hydrogen (see e.g. [11]). Oxygen functional groups have also been shown to play a role in physisorption of hydrogen on activated carbon: increasing oxidation of an activated carbon resulted in increased physisorption [12]. Graphitic carbon may be capable of dissociating hydrogen [13]; in fact, several groups have asserted that carbon nanotubes and nanofibers are capable of hydrogen dissociation and that this hydrogen in turn is able to intercalate the interlayer spacing of graphite nanofibers [14]. The effect of surface functionalities on hydrogen spillover to carbon has not been widely stud-

\* Corresponding author. Tel.: +1-814-863-6256;  
fax: +1-814-865-3248.

E-mail address: [lueking@psu.edu](mailto:lueking@psu.edu) (A.D. Lueking).

ied, but hydrogen spillover has been shown to chemically modify functional groups on carbon to form basic carbons [15]. Indeed, the wide variety of available carbon structures provides an interesting opportunity to systematically determine the effect of carbon properties, including pore size, graphitic content, and surface functionalities, on hydrogen spillover.

Mixing a catalytic material with a previously inert secondary material has been used to demonstrate hydrogen spillover [8]. As discussed by Conner and Falconer, this secondary spillover requires intimate contact between the two unlike materials and there may be an energy barrier to transfer hydrogen from one material to another [9]. Secondary spillover provides an interesting method to clearly delineate the role of carbon surface functionalities; maintaining the primary metal-carbon material and varying the secondary carbon establishes a constant hydrogen source to the secondary material. This eliminates several variables inherent to primary spillover, including doping efficiencies, carbon-metal interface, and metal content (see Fig. 1).

The objective of this work was to better understand how hydrogen spillover affects hydrogen storage on carbon materials. Secondary spillover experiments were used to act as a proof of concept of hydrogen spillover on carbon materials, and to determine the important parameters that affect hydrogen spillover. First, the carbon materials were characterized in terms of physical and chemical properties in order to extend this information to hydrogen spillover; hydrogen uptake was also measured for undoped carbons at ambient conditions to serve as a baseline for subsequent doping experiments. Secondly, carbons were doped with metals in an attempt to optimize a carbon-metal system and find a promising material for hydrogen storage goals; variables studied included metal, metal doping technique, and carbon support. Finally, a common hydrogen spillover source was used to isolate the role of a secondary carbon material in secondary

spillover studies; the effects of doping ratio, carbon type, and pressure on hydrogen spillover were explored. The underlying theme behind these objectives was to understand the chemical properties favorable for hydrogen spillover in order to develop a new hydrogen storage material; thus the experimental design focused on equilibrium rather than rate studies. Likewise, the measurements were made at ambient conditions (up to 1 bar and 300 K) in order to screen materials and understand trends; the storage capacities of these materials at pressures relevant for hydrogen storage applications will be reported in future work.

## 2. Methods

### 2.1. Carbon nanofiber preparation

All synthesis gases were obtained from cryogenic gases and had the following purities: Matheson grade methane (99.99%), CP grade ethylene (99.5%), pre-purified grade helium (99.8%), and ultra-high purity hydrogen (99.999%).

Single-wall carbon nanotubes (SWNTs) were produced catalytically using an iron-molybdenum catalyst supported with a hybrid alumina-silica material, as described by Cassel et al. [16]. Graphite nanofibers (GNFs) were synthesized by passing a 1:4 ethylene:hydrogen mixture over a 7:3 iron:copper catalyst at 600 °C; these conditions have been shown to produce herringbone GNFs [17]. Multi-walled carbon nanotubes (MWNTs) were synthesized using a  $\text{Ni}_{0.4}\text{Mg}_{0.6}\text{O}$  catalyst at 650 °C, as developed by Chen et al. [18]. Two separate acid treatments were used to remove the synthesis catalyst from the GNFs and MWNTs: fibers were either mixed with 6N  $\text{HNO}_3$  or 1N  $\text{HCl}$  for 24 h at a ratio of 50 ml acid/g catalyst. Also, one sample of MWNTs was washed in 6N  $\text{HNO}_3$  three times, as previous work shows that one acid treatment may be insufficient to remove the synthesis

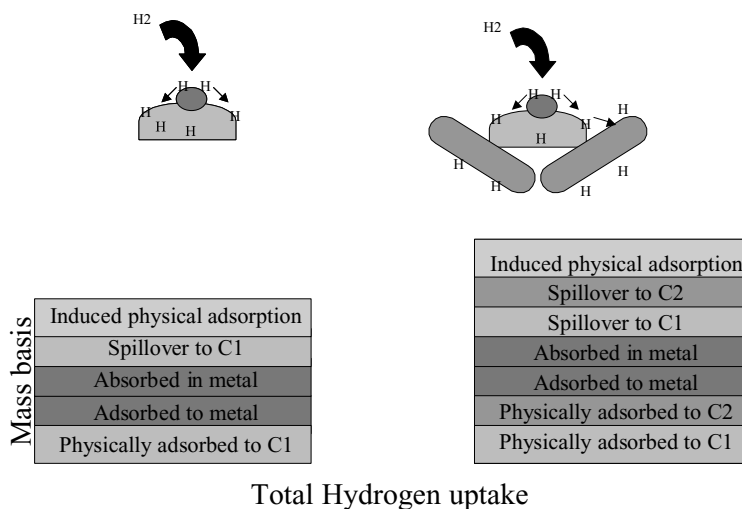


Fig. 1. Schematic comparing primary to secondary spillover and how each component contributes to overall hydrogen uptake. Here, C1 refers to the primary carbon and C2 refers to the secondary carbon.

catalyst [1,2] and EDX determinations (data not shown) indicated that subsequent acid treatment significantly reduced the catalyst content of the MWNTs to less than 1%. The SWNT were treated with 48% HF (Aldrich) to remove the silica-alumina support.

BPL activated carbon ( $12 \times 30$  mesh), activated carbon fibers (ACF) (Osaka Gas) were used for comparison to the carbon nanofibers. A super-activated AX-21 carbon with enhanced dehydration and both high temperature (ArcHT) and low temperature (ArcLT) finishing processes was obtained from Arcanum Corporation. The activated carbon (BPL-AC) was demineralized in a method analogous to that used for the carbon nanofibers, with either a 6N HNO<sub>3</sub> or a 1N HCl solution; the ACF and AX-21 were not expected to have significant ash content, and were thus used as received.

## 2.2. Supported catalysts

Commercially prepared catalysts included platinum and palladium supported on activated carbon, Pt/C 1600, Pt/C 1680, and Pd/C 1890 (STREM Chemicals). Other supported catalysts were prepared by either incipient wetness impregnation or a reflux method in ethylene glycol, as described by Satishkumar et al. [19]. The precursor metals were 5% Pd(NH<sub>3</sub>)<sub>2</sub>(NO<sub>2</sub>)<sub>2</sub> and 5% Pt(NH<sub>3</sub>)<sub>2</sub>(NO<sub>2</sub>)<sub>2</sub> solutions (STREM Chemicals), both metals were diluted to a 1% solution prior to use. The amount of metal on the surface,  $M_S$ , was estimated by the hydrogen isotherm extrapolation method introduced by Benson and Boudart [20] in which the hydrogen isotherm from low pressures (0.07–0.3 bar) is extrapolated to zero pressure to determine the monolayer surface coverage of the catalyst:

$$Q_M = \lim_{P \rightarrow 0} Q_T \quad (1)$$

where  $Q_M$  is the uptake by the metal and can include adsorption and/or absorption,  $Q_T$  is the total hydrogen uptake of the material, including both the metal and carbon (primary and/or secondary). This extrapolated value was then used to calculate the atoms of metal on the surface per gram of material, assuming that each surface metal atom interacted with one hydrogen atom (e.g.  $H/M_S = 1$ ). This value of  $M_S$  was then used in calculation of metal dispersion, by comparing to the metal content, as determined by neutron activation analysis.

For secondary spillover studies, physical mixtures of supported catalysts and a secondary carbon were prepared by grinding the two carbons with a mortar and pestle in a predetermined ratio. The metal to carbon ratio was varied to determine the effect of mixing ratio on hydrogen surface density. In subsequent secondary spillover studies, a constant ratio of one part metal–primary carbon to nine parts secondary carbon was used. The mixtures were then calcined in situ at 400 °C for 2 h before hydrogen reduction and adsorption studies.

## 2.3. Characterization

The metal composition for the carbon nanofibers was measured using neutron activation analysis (NAA) using P-tube irradiation for magnesium, copper, and aluminum analysis and in-core irradiation for nickel, iron, and molybdenum. Standard methods for BET surface area and pore size analysis of the carbon materials were characterized using a Micromeritics ASAP 2000 with nitrogen at 77 K. Prior to surface area analysis, the samples were degassed at 150 °C in a vacuum. The carbon nanofibers were examined with a Phillips XL30 FEG scanning electron microscope (SEM). Surface functionalities were characterized using standard Boehm titrations. Samples of the carbon fibers were equilibrated for 24 h with 0.05N solutions of HCl, NaHCO<sub>3</sub>, Na<sub>2</sub>CO<sub>3</sub>, and NaOH. The supernatant was then back-titrated to determine the equivalents that had been neutralized with the different solutions. It is generally accepted that NaHCO<sub>3</sub> titrates carboxyl groups, Na<sub>2</sub>CO<sub>3</sub> titrates carboxyl and lactone groups, while NaOH titrates carboxyl, lactone, and phenolic functional groups [21]. The specific chemical nature of groups titratable by HCl is less established, but these groups would be of basic character.

## 2.4. Adsorption experiments

Hydrogen uptake was determined using static volumetric measurements on a Micromeritics ASAP 2000 with a relative equilibrium tolerance set at 5.0%. A preliminary error propagation analysis indicated that the sensitivity of the instrument was sufficient to differentiate between different sorbents under ambient conditions; reproducibility of samples and quality checks confirmed this conclusion. The sample cell in the measurement was modified to allow in situ pretreatment of the sample with flowing gases. Prior to adsorption measurements, samples were reduced for 6 h in 40 cc (STP)/min hydrogen gas at 250 °C and then degassed at 400 °C for at least 8 h. Adsorption experiments were conducted at 300 K and pressures up to 1 bar. Typically, 50–100 mg of sample were used in the experiments. The hydrogen monolayer coverage was calculated by extrapolating to zero pressure, as described by Eq. (1).

In order to compare the degree of hydrogen spillover between carbons, an enhancement factor,  $\eta$ , was defined as:

$$\eta = \frac{Q_C}{Q_{C'}} \quad (2)$$

where  $Q_C$  denotes the uptake of the carbon when mixed with a supported catalyst and  $Q_{C'}$  denotes the uptake of the carbon measured with no catalyst. For calculation of  $Q_C$ , the contribution of each component to hydrogen uptake was assumed to be independent of the presence of other components:

$$Q_C = Q_T - Q_{M+Cl} \quad (3)$$

where  $Q_T$  is the total hydrogen uptake of the composite material,  $Q_{M+C1}$  is the hydrogen uptake of the primary supported catalyst, and  $Q_C$  is the uptake attributed to the secondary carbon. The enhancement term,  $\eta$ , reflects any changes in hydrogen uptake in a carbon upon mixing with a supported catalyst that acts as a hydrogen source. Inherent in Eq. (3) is an assumption of equilibrium—that the uptake of the primary supported catalyst,  $Q_{M+C1}$ , is unchanged upon mixing with a secondary carbon.

### 3. Results and discussion

#### 3.1. Carbon: preliminary characterization

The carbons examined included carbon nanomaterials (SWNT, MWNT, GNF), activated carbon (BPL AC), activated carbon fiber (ACF), and a super activated carbon AX-21 (Arc HT, ArcLT). The carbons exhibited BET surface areas ranging from 45 to 2400 m<sup>2</sup>/g (Table 1). Surface functionalities, as evidenced by titratable functional groups, were highly variable for the carbons in the study (Table 1). Treatment in an oxidizing acid, such as 6 M HNO<sub>3</sub> introduced additional functional groups compared to treatment in 1 M HCl, as evidenced for MW and BPL AC (Table 1).

Hydrogen adsorption of the undoped carbons,  $Q_C'$ , was measured at the same conditions as subsequent measurements on doped carbons, such that the level of enhancement upon the addition of a catalytic hydrogen source could be calculated by Eq. (2). The magnitude of hydrogen uptake ranged from 0.43 cm<sup>3</sup>/g (STP) to 3.8 cm<sup>3</sup>/g (STP). Previous studies at cryogenic conditions (77 K, 1 bar) showed a stronger dependence upon surface area for carbons [22]; however this is due to the difference in adsorption conditions (300 K versus 77 K). As physisorption of hydrogen on carbon is expected to be negligible at room temperature conditions, the uptake measurements were used primarily for calculation of the enhancement factor for secondary spillover studies.

There was a wide variation in the hydrogen uptake for SWNT at ambient conditions, and this seemed to be dependent upon synthesis conditions (Table 1). High-yield SWNT (SW-HF-2) had a hydrogen uptake comparable to the other carbons, whereas a low yield SWNT sample (SW-HF-1) had a three-fold increase in hydrogen uptake at ambient conditions. A difference in carbon reaction time led to a difference in yield and carbon content. Thus, the difference in hydrogen uptake for these two samples could be due to differences in residual metal content, but subsequent attempts to remove metals via acid dissolution did not significantly alter the ambient hydrogen uptake of these samples (Table 1). This implies that either encapsulated metal may alter hydrogen uptake or there is some inherent difference in the SWNT properties; these variations for SWNT synthesis conditions is currently under investigation. However, the introduction of an enhancement factor (Eq. (2)) in this study for the secondary spillover studies allowed comparison between carbons with different initial (undoped) ambient hydrogen uptake.

#### 3.2. Primary spillover: optimization of a catalyst-carbon system

The primary supported catalysts in this study consisted of supported platinum or palladium on carbon. Carbon nanomaterials were doped via either incipient wetness or reflux doping, and these materials were compared to commercially available counterparts (platinum or palladium supported on activated carbon). Both total hydrogen uptake and calculated metal dispersion were used to evaluate the different metal-carbon combinations and doping methods. The purpose was to screen catalyst-carbon materials and doping methods for later application in high-pressure experiments leading to a commercially viable hydrogen storage material. A high metal dispersion indicates effective doping, and this is expected to lead to increased hydrogen spillover. In addition, the hydrogen uptake of the supported catalysts was used for calculation of an enhancement factor for secondary

Table 1  
Characterization and Hydrogen uptake of various carbon fibers

Carbon	Acid treatment	BET SA (m <sup>2</sup> /g)	HCl titratable (μeq/g)	NaHCO <sub>3</sub> titratable (μeq/g)	Na <sub>2</sub> CO <sub>3</sub> titratable (μeq/g)	NaOH titratable (μeq/g)	$Q$ @1 bar (cm <sup>3</sup> /g)
SW-HF-1 <sup>a</sup>	48% HF	505					3.0
SW-HF-2 <sup>a</sup>	48% HF	372	0	340	590	650	0.98
MW-HNO <sub>3</sub>	6 M HNO <sub>3</sub>	76	1600	300	610	630	0.43
MW-HCl	1 M HCl	77	330	450	550	1200	1.1
GN-HNO <sub>3</sub>	6 M HNO <sub>3</sub>	77	86	200	220	740	1.2
GN-HCl	1 M HCl	45					1.2
BPL AC-HNO <sub>3</sub>	6 M HNO <sub>3</sub>	1030	670			1600	1.3
BPL AC-HCl	1 M HCl	1120	530			1100	1.1
Aactivated carbon fiber	None	2000	370	BDL	430	490	1.3
AX-21, ArcHT	None	2380	1000	BDL	570	810	2.1
AX-21, ArcLT	None	2400	700	460	1300	1200	1.6

<sup>a</sup> Sample size limited analysis of these fibers by titration method.

Table 2  
Characterization of doped carbon materials and primary spillover results

Class	Name	Metal content (g/g)	Metal dispersion (%)	$Q$ @1 bar (cm <sup>3</sup> /g)	H:M <sub>S</sub> @1 bar	H:M <sub>T</sub> @1 bar
Commercial	Pt/C 5% (1600)	5.0%	11%	2.3	7.3	0.81
	Pt/C 5% (1680)	5.0%	9.4%	1.2	4.5	0.42
	Pt/C 10%	10%	6.6%	1.0	2.8	0.18
Doped-Pt/Arc <sup>a</sup>	Pt/Arc 1% incipwet	1.4%	17%	2.0	15	2.6
	Pt/Arc 1% reflux	0.5%	64%	4.3	23	15
	Pt/Arc 5% incipwet	6.0%	38%	3.4	2.6	0.99
Commercial	Pd/C	5.0%	59%	4.1	1.3	0.78
Doped-Pd/Arc <sup>a</sup>	Pd/Arc 0.1% reflux	0.06%	E <sup>b</sup>	2.3	22	36
	Pd/Arc 1% incipwet	1.8%	67%	3.1	2.5	1.7
	Pd/Arc 1% reflux	3.1%	57%	4.5	2.4	1.4
	Pd/Arc 5% reflux	14%	48%	9.7	1.4	0.66
Doped-Pd/SW	Pd/SW 5% reflux	5.7%	E <sup>b</sup>	13	1.4	2.2
Doped-Pd/MW	Pd/MW 5% reflux	0.6%	E <sup>b</sup>	2.6	3.2	4.3

<sup>a</sup> Arc: AX-21 super activated carbon.

<sup>b</sup> The calculated metal dispersion exceeded 100% in several cases, and this is discussed as a limitation of the extrapolation method to calculate surface metal when hydrogen spillover is possible.

spillover studies, in a method analogous to the undoped carbons.

In general, doping of carbon nanomaterials significantly increased the hydrogen uptake compared to the commercially available material, in terms of both H:M ratios and uptake per unit mass (Table 2, Fig. 2). For platinum doped

carbons, the metal dispersion increased significantly (from 6.6–11% to 64%) with reflux doping, indicating a better utilized metal compared to commercially available carbons or those doped via incipient wetness (Table 2). Of the supported catalysts studied, the palladium supported on SWNTs had the highest uptake with 13.10 cm<sup>3</sup> (STP)/g; palladium

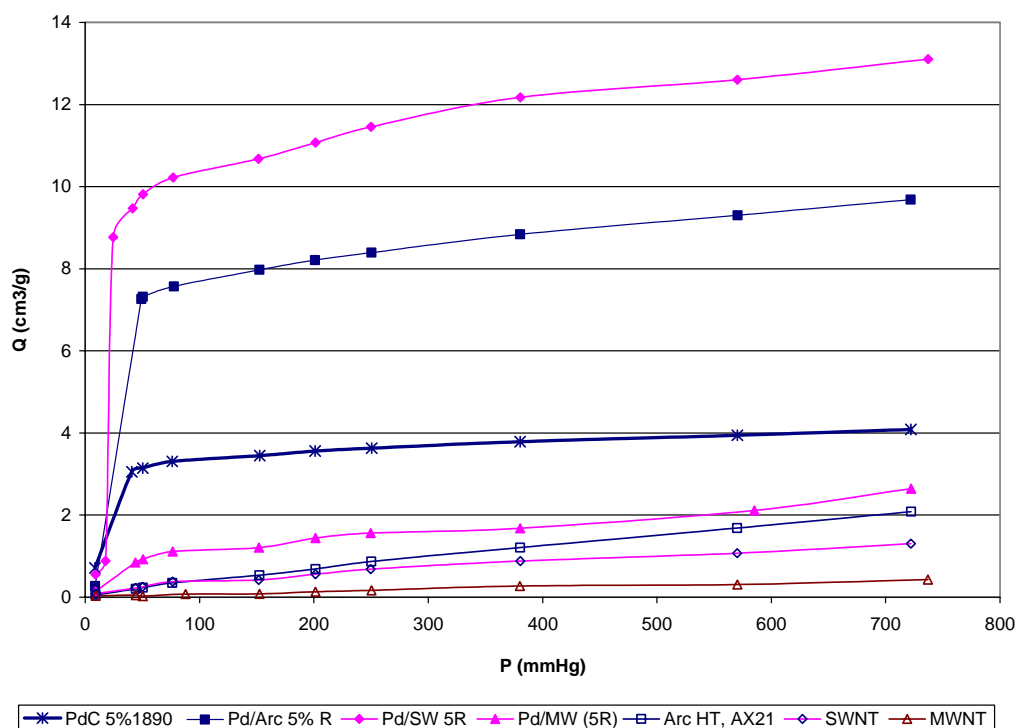


Fig. 2. Hydrogen uptake for different primary metal-carbon systems compared to the corresponding undoped carbons. Reflux doping SWNT with palladium (Pd/SW(5) 5% R) resulted in the highest hydrogen uptake per gram when compared to both commercial palladium-carbon materials (PdC 5% 1890) and palladium doped on a super activated carbon under the same conditions (Pd/Arc 5%R). The closed symbols represent the doped material whereas the open symbols represent the uptake of the undoped carbon. Arc denotes super activated carbon AX-21.



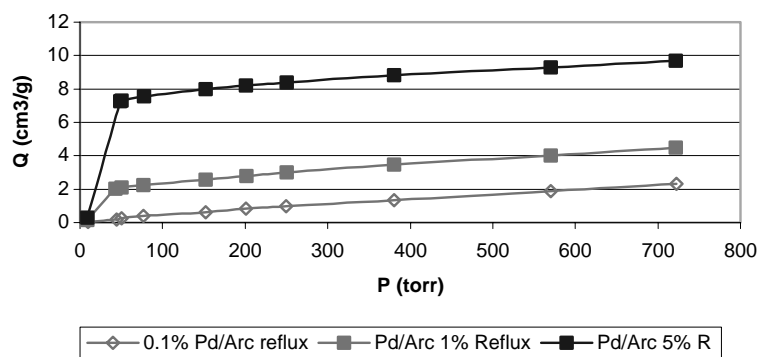


Fig. 3. Hydrogen uptake for different primary metal-carbon systems with decreasing metal content. Attempts to reduce the palladium content successfully increased the H:M ratio, but did not result in an enhanced total hydrogen uptake (per gram).

supported on the super activated carbon (Pd/Arc-5R) had an uptake of  $9.7 \text{ cm}^3 \text{ (STP)/g}$  (Table 2 and Fig. 2). These values correspond to  $\sim 0.1\%$  hydrogen uptake by weight at a pressure of 1 bar. Attempts to reduce the palladium content were successful in increasing the H:M ratio, but the overall hydrogen uptake was reduced (Table 2, Fig. 3). This result highlights the difference between assessing hydrogen uptake in terms of H:M versus weight percent. Comparison of the results here to similar hydrogen spillover experiments with platinum-loaded carbon fibers show that the reflux doping method is promising in terms of H:M<sub>T</sub> ratios [23]. However, the metal content was not easily controlled for the reflux doping, and the metal content measured by neutron activation analysis indicated that not all of the added metal ended up on the surface of the carbon (Table 2).

### 3.3. Primary spillover—validity of assumptions

The metal dispersion for several supported catalysts (e.g. Pd/Arc 0.1% R, Pd/SW 5% R, and Pd/MW 5% R) calculated from the extrapolation method of Benson and Boudart, exceeded 100% (Table 2). These results suggest that there are certain limitations to the Benson–Boudart extrapolation method for determining metal dispersion, despite its prevalent use in the literature. This extrapolation method was first developed when hydrogen isotherms of supported metals were observed to be parallel to the hydrogen isotherm of the support; this observation led to the conclusion that the difference between the two isotherms was due to monolayer coverage of the catalyst. Simply stated, this method assumes that the surface of the metal becomes saturated instantaneously with exposure to the adsorbate at low pressures and that physisorption of the support is negligible. However, for parallel isotherms to be observed, hydrogen spillover must be negligible for the system. This is clearly not the case for several of the combinations observed in this study.

There are no caveats to the use of the Benson and Boudart extrapolation method for hydride forming metals such as palladium. The assumption of instantaneous surface coverage would be valid for hydride forming metals, if the hy-

drides were formed at low pressures. However, comparison of the palladium to platinum doped systems shows: (1) the calculated metal dispersion for the commercially available supported catalysts was quite different for the two metals: 7–11% for platinum on activated carbon compared to 59% for palladium on activated carbon; (2) metal dispersions greater than 100% were observed only for palladium containing materials; and (3) the extrapolated H:M<sub>s</sub> appeared to be dependent on the given palladium doping level (e.g. 1 or 5%) rather than the total metal content. These observations indicate that caution must be used when using the extrapolation method to calculate metal dispersion when there is the possibility of hydride formation, and will be addressed in future modeling studies.

### 3.4. Secondary hydrogen spillover

Secondary spillover provides an opportunity to isolate how the physical and chemical properties of carbon accept spillover hydrogen. Unlike primary spillover studies, where the material performance is dependent upon factors such as efficiency of metal doping, dispersion, and the resulting carbon-metal interface, secondary spillover effectively reduces the number of experimental variables. A catalyst supported on a primary carbon provides a constant “hydrogen source” for a given secondary carbon receptor. This allows isolation of the effects of the secondary carbon material. The effects of secondary spillover are illustrated in Fig. 4: mixing undoped SWNT (secondary carbon) with palladium supported on SWNT (primary carbon) shows an increased uptake for the composite material compared to the weighted average of the materials measured separately. Fig. 4 graphically illustrates how the introduction of a hydrogen source leads to an enhancement of the hydrogen uptake for a given carbon. Careful analysis of Fig. 4 suggests that the enhancement in hydrogen uptake for the composite material is a function of pressure; this will be discussed in more detail below. For simplicity, the enhancement factor is reported at 1 bar pressure for a mixing ratio of 1 part supported catalyst to 9 parts carbon, unless otherwise noted.

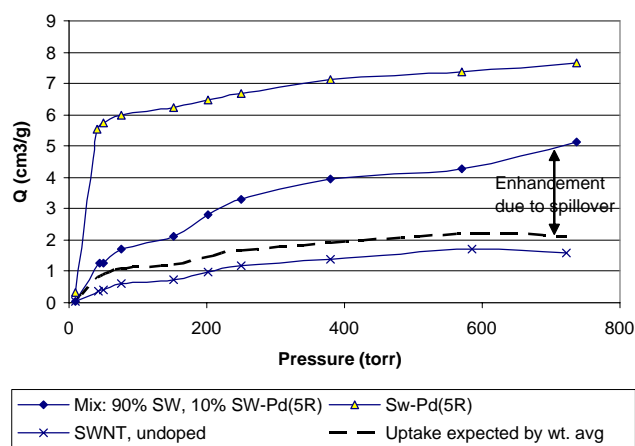


Fig. 4. Effect of secondary spillover on hydrogen uptake. Physical mixing of SWNTs with palladium-doped SWNTs (Sw/Pd-5R) resulted in enhancement in hydrogen uptake of the system due to secondary spillover. The line denoted as “uptake of separate components” is a weighted average of the materials, as measured separately.

### 3.5. Variation of mixing ratio to develop spillover conceptualization

Commercially available Pt/C 1600 was mixed with the secondary carbon MWNT to investigate the effect of mixing ratio on secondary hydrogen spillover. When the supported catalyst to secondary carbon mixing ratio was varied from 1:99 to 1:9, the total hydrogen uptake of the composite material was optimized at a mixing ratio of 1 part Pt/C to 19 parts MWNT (Table 3). Srinivas and Rao found similar results in that varying the mixing ratio of a supported catalyst with carbon led to an optimum ratio for hydrogen uptake, whereas carbon monoxide adsorption decreased with decreased supported catalyst content [8].

This dependence of hydrogen uptake on mixing ratio is the basis for the following common conceptualization of hydrogen spillover: as a secondary receptor (i.e. MWNT) is added to the system, the secondary carbon is able to uptake spillover hydrogen and the overall uptake is increased. At some point, the secondary carbon content increases beyond the point where the supply of spillover hydrogen is sufficient and the overall hydrogen uptake is reduced. At high dilution of the hydrogen source (Pt particles in the case of Pt/C 1600) the supply of hydrogen to the secondary carbon is negligible

compared to that expected for the secondary carbon alone. In effect, changing the “distance” between hydrogen sources and acceptors shifts the balance between the rate of hydrogen flux from the catalyst and recombination of the hydrogen atoms on the surface.

### 3.6. Pressure dependence of hydrogen spillover

Hydrogen spillover is generally thought to be proportional to the square root of pressure, however this common assumption is based on Langmuir’s model and not directly linked to experimental data. Furthermore, it has not been demonstrated that hydrogen spillover will not occur at very low pressures, which is the common assumption tied to the extrapolation method of Benson & Boudart, as discussed above. Rather, hydrogen spillover as a surface phenomenon should relate directly to surface concentration gradients and only indirectly to hydrogen pressure. To illustrate this point, the pressure dependence of the previous series—MWNT mixed with Pt/C at various dilution ratios—was analyzed. The enhancement of hydrogen uptake was found to be a function of pressure with the greatest enhancement found at pressures less than 200 Torr (Fig. 5). The pressure dependence of the enhancement factor exhibited a bimodal dependence with local maxima at 50 and 150 Torr (Fig. 5). The relative intensity of these two peaks was dependent upon mixing ratio: the 50 Torr peak gradually decreased with increasing catalyst content whereas the peak at 150 Torr generally reflected the hydrogen uptake. With a mixing ratio that resulted in a high concentrations of Pt/C (1:9), the bimodal nature was less pronounced. There are several possible explanations for this behavior, and these will be explored with further modeling studies. However, this illustrates that simple equilibrium modeling is insufficient to explain this behavior, as will be discussed more in a subsequent section.

### 3.7. Carbon properties and hydrogen spillover

Here, carbons from several different sources were analyzed through the use of a secondary spillover analysis in which both the primary catalyst and secondary carbon were varied. The first result of note is that the hydrogen uptake tends to be clustered in terms of secondary carbon (Fig. 6), and this supports the assertion that this type of analysis reduces differences in the primary catalyst.

The enhancement factor provides an indication of the synergistic (or lack thereof) effects of mixing. Comparison of these effects by carbon group provides some indication of factors that are beneficial or detrimental to hydrogen uptake, and how these factors can be controlled and optimized. In most cases, the addition of a secondary carbon increased the total hydrogen uptake of the mixture when compared to the separate components ( $\eta > 1$ ) similar to that illustrated in Fig. 6. The greatest enhancement was observed for SWNTs and MW-HNO<sub>3</sub> with enhancement factors of 3, indicating

Table 3  
Effect of dilution ratio on hydrogen uptake

Parts MW	Parts Pt/C 1600	$Q_{\text{r H}_2}$ (cm <sup>3</sup> /g STP) <sup>a</sup>	$\eta_{\text{H}_2}$ <sup>a</sup>
0	100	1.7	
9	1	1.0	1.7
19	1	1.3	2.7
49	1	0.80	1.7
99	1	0.35	0.73
100	0	0.43	

<sup>a</sup> Measured at 1 bar, 300 K.

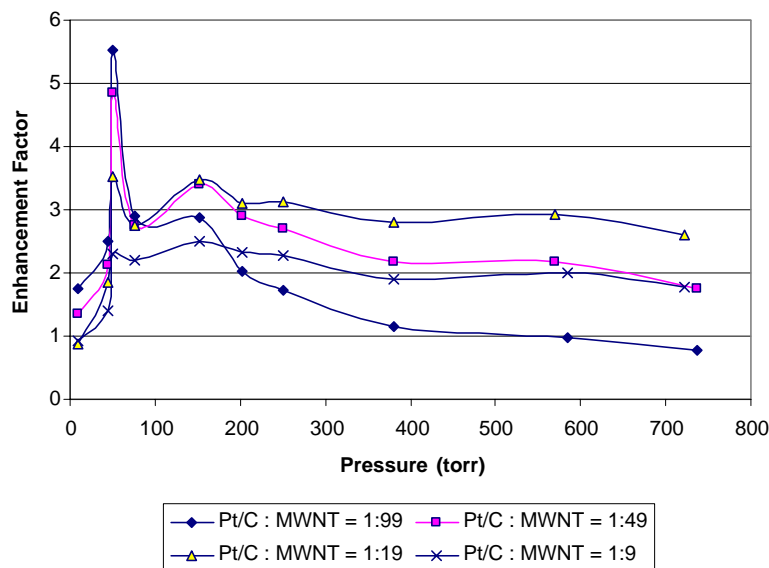


Fig. 5. Enhancement factor (see Eq. (2)) as a function of pressure for selected mixtures of a supported catalyst with the secondary carbon, MWNT. The enhancement factor is one measure of hydrogen spillover, and is defined as the ratio of hydrogen uptake when the carbon is mixed with a supported catalyst to that measured separately for the undoped carbon.

that the uptake of the carbon could be increased by a factor of 3 upon the introduction of a hydrogen source.

In several other cases, the addition of a hydrogen source to a secondary carbon not only did not result in an enhancement (e.g. when  $\eta \sim 1$ , as in the case of several ArcHT samples), but combination of two materials actually *suppressed* the uptake of the composite compared to the individual components. The enhancement factor was less than 80% of the weighted average of the materials separately for several GNF samples and all BPL activated carbon samples tested (Table 4). Whereas no enhancement can be easily be explained away by insufficient contact between the primary and secondary carbon, suppression indicates that the presence of a secondary carbon reduces the uptake of the catalyst and the primary carbon. This could result if the secondary carbon led to poisoning of the catalyst such that the hydrogen source is blocked, e.g. by carbon migration; this effect

was observed by Boudart et al. in their study of hydrogen spillover on tungsten carbides [24], and certainly cannot be ruled out here. However, the observation of suppressed hydrogen uptake may arise due to the data analysis based on an equilibrium assumption, and this is explained in more detail further.

Despite the grouping of hydrogen uptake based on secondary carbon (Fig. 6), no clear trend emerged between surface functionalities and secondary spillover. This is likely due to the wide variation in source material and competing factors such as differences in microporosity. Previous trends related to functional groups have utilized chemical treatment of a single carbon source material to elucidate trends between adsorption and surface functional groups [12,25,26] and here, this demonstrates the possibility for future work. Many previous hydrogen spillover studies have focused primarily on spillover to metal oxide supports [11,12], however the preliminary analysis here gives no indication that hydroxyl groups are necessary to accept spillover hydrogen. The suppression effect ( $\eta < 0.8$ ) did appear to be dependent upon secondary carbon receptor, with this observed only for GNF and BPL activated carbon (Table 4).

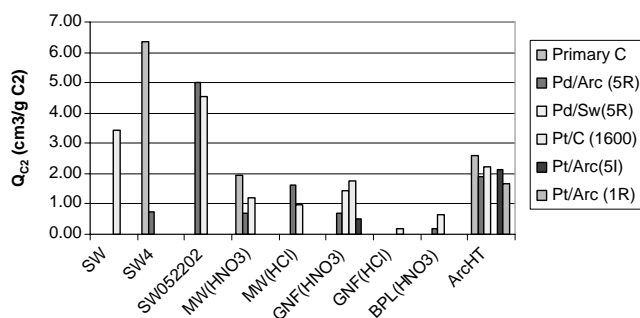


Fig. 6. Hydrogen uptake (per gram of secondary carbon) for secondary carbons after mixing with a supported catalyst tended to cluster based on type of secondary carbon, independent of the catalyst used. The secondary carbon is plotted along the x-axis. The hydrogen uptake of the secondary carbon,  $Q_{C2}$ , is calculated based on the analysis described in the methods section.

### 3.8. Spillover conceptualization and modeling needs

The existing data treatment is based on a simple additive analysis in which the assumption is made that the addition of a secondary carbon will not affect the uptake of the primary carbon and/or supported catalyst. This assumption is commonly used in analysis of composite material and is based on an equilibrium interpretation which presupposes that there exists a unique hydrogen uptake for a given temperature and pressure, and this uptake will be unaffected



Table 4

Secondary spillover for various primary catalyst/secondary carbons at a mixing ratio of 1 part primary catalyst to 9 parts secondary carbon

Carbon type	$Q$ @1 bar ( $\text{cm}^3/\text{g}$ )					Enhancement due to spillover @ 1 bar, $\eta = Q_{\text{C}}/Q_{\text{C}}'$				
	Pd/Arc (5R)	Pd/SW (5R)	Pt/C (1600)	Pt/Arc (5I)	Pt/Arc (1R)	Pd/Arc (5R)	Pd/SW (5R)	Pt/C (1600)	Pt/Arc (5I)	Pt/Arc (1R)
SW-HF-1			3.7					1.2		
SW-HF-4	4.4					1.3				
SW-HF-5	5.8	5.1				3.2	2.9			
MW( $\text{HNO}_3$ )	1.9	2.1	1.3			1.6	2.8	2.8		
MW( $\text{HCl}$ )	2.9	1.8				1.4	0.87			
GNF( $\text{HNO}_3$ )	1.8	2.0	1.9	0.86		0.58	1.2	1.5	0.44	
GNF( $\text{HCl}$ )			0.26					0.15		
BPL( $\text{HNO}_3$ )	1.7	1.7				0.15	0.50			
ArcHT	3.0	2.7		2.3	2.1	0.90	1.1		1.0	0.80

Pd- and/or Pt-doping on Superactivated carbon, AX-21 (Arc), SW (SWNT); Pt/C 1600 is a commercially prepared catalyst obtained from Aldrich. R refers to doping via reflux, whereas I refers to doping via incipient wetness. See Section 2 section for a further explanation of the enhancement factor.

by an additional hydrogen “sink”. Specifically, imbedded in Eq. (3) is the calculation of a ‘new’ hydrogen uptake of the secondary carbon,  $Q_{\text{C}}$ , based on a previous measurement of  $Q_{\text{M+C1}}$ . Thus, Eq. (3) allows for variation in the uptake of the secondary carbon upon mixing, but not of the primary carbon or supported metal ( $Q_{\text{M+C1}}$ ). Although this is somewhat intuitive, three observations above indicate that this type of analysis is insufficient to describe the system: (1) the existence of an optimum mixing ratio; (2) the pressure dependence of hydrogen spillover; and (3) the suppression of overall hydrogen uptake for certain systems upon mixing.

These three observations can be explained only by a steady-state analysis. Although common equilibrium models allows transfer through use of rates of adsorption and desorption, the net flux in an equilibrium system is zero. In other words, the rate of adsorption equals the rate of desorption. In a hydrogen spillover system, there is no overall net flux as the concentrations may remain constant, but there is a net flux from the supported metal to the carbon surface (both primary and secondary carbons). Steady state, in a hydrogen spillover system, implies that the net rate of hydrogen dissociation and surface diffusion from the metal equals the net rate of recombination and desorption. However, unlike the equilibrium two-phase system, there is a net flux between certain system boundaries. Development of this steady-state model is underway, and will be used to explain the three observations above, as well as to explore the effects of temperature, pressure, catalyst concentration, and surface functionalities, in order to better design a material to utilize the hydrogen spillover phenomenon.

### 3.9. Implications of spillover to hydrogen storage

Residual metal content has been shown previously to affect hydrogen uptake measurement in carbon systems [1,2]. Efforts to remove residual catalyst may be insufficient [1,2]; the undoped SWNT suggested that even multiple acid treatments may not be sufficient to remove residual metals and/or encapsulated metals may affect hydrogen storage. Some previous studies have claimed that hydrogen spillover affects

only the rate of hydrogen uptake but not the overall capacity of a given material [27]. However, as observed for multiple carbon systems, the hydrogen uptake of a given material could be enhanced by as much as a factor of three at ambient conditions (Table 4). This enhancement was dependent upon the type of carbon, and was in some cases suppressed. In addition, a clear distinction must be made between the total hydrogen uptake on a per mass basis and the degree of hydrogen spillover. For example, the enhancement factor of MWNT was high, but this could not counteract the effect of the low baseline adsorption of the MWNT such that the overall hydrogen uptake on a per mass basis remained lower than several other systems with a low enhancement factor. Thus, for optimization of hydrogen storage conditions, both physisorption and chemisorption must be considered, as is alluded to in Fig. 1.

Comparison of these results to other materials exhibiting hydrogen spillover, suggest several practical advantages for the doped SWNTs in this study. Previously, Lueking and Yang reported a MWNT sample containing residual NiMgO catalyst had an uptake of 0.6% by weight under ambient conditions [1], and was increased to 3.7% at a pressure of 69 bar [2]. The MWNT/NiMgO composite system required high temperature activation in hydrogen to fully activate the catalyst and/or modify the carbon-catalyst interface for hydrogen spillover [2]. Although the best uptake reported here ( $13 \text{ cm}^3/\text{g}$  for Pd/SW-5R, or equivalently 0.12%) is one-sixth of the value reported for the MWNT/NiMgO system, the pretreatment for these studies is much less severe ( $250^\circ\text{C}$   $\text{H}_2$ ) due to the different catalyst composition and activation requirements. Comparison of these two materials under similar pretreatment conditions showed that the hydrogen uptake for the MWNT/NiMgO system was significantly reduced when pretreated at lower temperatures ( $<0.1\%$ ). Lower pretreatment temperatures may be more desirable for commercial applications. The objective of this work was to better understand how hydrogen spillover affects storage rather than serve as an ultimate measure of hydrogen storage capacity. Thus, the overall hydrogen storage capacity reported here at 1 bar is not feasible for practical applications. The capacity

of these doped materials to store hydrogen at higher pressures, as well as the effect of pressure on hydrogen spillover, will be reported in future work.

#### 4. Conclusions

1. Increased hydrogen spillover does not necessarily result in the best overall hydrogen uptake. Therefore, the best process by which to optimize a hydrogen storage material is to start with the material best suitable for physisorption and then alter/dope this material using the conditions found for best hydrogen spillover.
2. Secondary spillover experiments effectively eliminated experimental variables associated with primary spillover. Five distinct primary carbon-metal systems were studied, and despite these different primary sources, the secondary spillover results were dependent upon the properties of the secondary carbon rather than the hydrogen source.
3. Models and/or adsorption isotherms that employ the equilibrium assumption of a unique surface concentration for a given temperature and pressure were insufficient to model the system in order to design and optimize materials. This was evidenced by (1) an optimal hydrogen uptake for dilution ratio; (2) the pressure dependence of hydrogen spillover; and (3) the suppression of overall hydrogen uptake for certain systems upon mixing. A steady-state reaction-surface diffusion model is needed to better understand and model hydrogen spillover.
4. Carbon nanotubes (SWNTs and MWNT) were the best acceptor of spillover hydrogen. The purity and synthesis of SWNTs played a key factor in hydrogen uptake, and this needs to be further explored. The hydrogen uptake for the Pd-doped SWNTs was  $\sim 0.1\%$  at 1 bar and 300 K. Although not practical for commercial applications, extension of this material to high-pressure conditions shows promise, especially due to relatively mild pretreatment conditions.

#### Acknowledgements

The authors would like to thank Leah Minc of the Michigan Memorial Phoenix Project for conducting the elemen-

tal analysis on the Ford Nuclear Reactor. Helmut Stern and John Getsoian of Arcanum Corporation provided the Arcanum AX-21 super activated carbon. This work was funded by NSF CTS-0138190.

#### References

- [1] A. Lueking, R.T. Yang, *J. Catal.* 206 (2002) 165.
- [2] A. Lueking, R.T. Yang, *AIChE J.* 49 (2003) 1556.
- [3] A.J. Robell, E.V. Ballou, M. Boudart, *J. Phys. Chem.* 68 (1964) 2748.
- [4] M. Boudart, A.W. Aldag, M.A. Vannice, *J. Catal.* 18 (1970) 46.
- [5] F.H. Yang, R.T. Yang, *Carbon* 40 (2002) 437.
- [6] U. Roland, T. Braunschweig, F. Roessner, *J. Mol. Catal. A Chem.* 127 (1997) 61.
- [7] W.C. Conner, J.L. Falconer, *Chem. Rev.* 95 (1995) 759.
- [8] S.T. Srinivas, P.K. Rao, *J. Catal.* 148 (1994) 470.
- [9] M. Boudart, M.A. Vannice, J.E. Benson, *Phys. Chem. N.F.* 64 (1969) 171.
- [10] R.B. Levy, M. Boudart, *J. Catal.* 32 (1974) 304.
- [11] M.A. Vannice, M. Boudart, J.J. Fripiat, *J. Catal.* 17 (1970) 359; J.G. Kim, J.R. Regalbuto, *J. Catal.* 139 (1993) 175.
- [12] R.K. Agarwal, J.S. Noh, J.A. Schwarz, P. Davini, *Carbon* 25 (1987) 219.
- [13] Y. Ishikawa, L.G. Austin, D.E. Brown, P.L. Walker Jr., *Chem. Phys. Carbon* 12 (1975) 39.
- [14] D.J. Browning, M.L. Gerrard, J.B. Lakeman, I.M. Mellor, R.J. Mortimer, M.C. Turpin, *Nano Lett.* 2 (2002) 201.
- [15] J.A. Menendez, L.R. Radovic, B. Xia, J. Phillips, *J. Phys. Chem.* 100 (1996) 17243.
- [16] A.M. Cassell, J.A. Raymakers, J. Kong, H. Dai, *J. Phys. Chem. B.* 103 (1999) 6464.
- [17] N. Krishnakutty, C. Park, N.M. Rodriguez, R.T.K. Baker, *Catal. Today* 37 (1997) 295.
- [18] P. Chen, H.-B. Zhang, G.-D. Lin, Q. Hong, K.R. Tsai, *Carbon* 35 (1997) 1495.
- [19] B.C. Satishkumar, E.M. Vogl, A. Govindaraj, C.N.R. Rao, *J. Phys. D Appl. Phys.* 29 (1996) 3173.
- [20] J.E. Benson, M. Boudart, *J. Catal.* 4 (1965) 704.
- [21] H.P. Boehm, *Carbon* 32 (1994) 759.
- [22] M.G. Nijkamp, J.E.M.J. Raaymakers, A.J. van Dillen, K.P. de Jong, *Appl. Phys. A.* 72 (2001) 619.
- [23] J. Ozaki, W. Ohizumi, A. Oya, M.J. Illan-Gomez, M.C. Roman-Martinez, A. Linares-Solano, *Carbon* 38 (2000) 775.
- [24] M. Boudart, J.S. Lee, K. Imura, S. Yoshida, *J. Catal.* 103 (1987) 30.
- [25] P. Davini, *Carbon* 28 (1990) 565.
- [26] X.S. Zhao, G.Y. Cai, Z.Z. Wang, Q.X. Wang, Y.H. Yang, J.S. Luo, *Appl. Catal. B.* 3 (1994) 229.
- [27] K. Fujimoto, K. Masamizu, S. Asaoka, T. Kunugi, *J. Chem. Soc. Jpn.* 7 (1976) 1062.